Testing the effects of ultraviolet radiation on biological samples using laser interferometry

G. Frausto-Rea and M. del S. Hernández-Montes

Centro de Investigaciones en Óptica, A.C.,
Loma del Bosque 115, Col. Lomas del Campestre, León, Guanajuato, 37150, México.

Received 13 October 2025; accepted 27 July 2026

Laser interferometry is used to analyze biological samples non-invasively before and after exposure to ultraviolet B (UVB) radiation. The objective is to ascertain the damage induced by this type of radiation by quantifying displacements across the entire surface of the samples. The analysis of those displacements, with a resolution of a few micrometers, is presented. Displacements are induced by applying a sound load to the sample with and without radiation. The results are displayed as fringe patterns and displacement maps, where changes caused by UVB radiation exposure can be observed. It was found that displacement values decrease and fringe patterns change slightly due to the radiation. Displacement data is useful as it is an indicator of the biological sample's elasticity. This work contributes to the understanding of the impact of UVB irradiation on sample elasticity, which can be assessed non-invasively.

Keywords: Radiation; ultraviolet; laser interferometry; fringe patterns; displacements.

DOI: https://doi.org/10.31349/RevMexFis.72.061301

1. Introduction

The sun energy, or solar energy, which is present on Earth as electromagnetic radiation. The electromagnetic spectrum encompasses different wavelengths, which can be divided mainly into visible (400 to 700 nm), infrared (750 nm to 1 mm), and ultraviolet (200 to 400 nm), the latter of which is considered in this paper. In turn, the ultraviolet range can be divided into three types: UVA, UVB, and UVC. In the case of UVC and much of the UVB spectrum, radiation is absorbed by the atmosphere ozone layer. However, UVA radiation passes through the ozone layer and reaches the Earth's surface. Due to the deterioration of the ozone layer in recent years [1-4], there has been an increase in UVB radiation on Earth, leading to various problems for living beings [5-7]. Alterations in mechanical properties due to exposure to ultraviolet radiation have been demonstrated in synthetic materials and biological tissues. Some studies have shown that in both natural and synthetic materials, such as Glass/polyester composite, poly methyl methacrylate (PMMA), epoxy laminate, and elastic material, among others, distinct changes in their mechanical properties can be attributed to UV radiation [8-12]; for example, in the case of PMMA, exposure to ultraviolet light caused surface damage that made mechanical parameters degrade, as was the case of strength and strain at rupture [13]. Regarding biological tissues, specifically porcine skin, samples were subjected to two different doses of UV radiation which were high and lasted for prolonged periods, and were then analyzed to obtain the rigidity coefficients before and after radiation, resulting in a loss of skin elasticity [14]. Focusing on humans, high exposure to UVB rays can cause various skin problems, such as premature aging, darkening or burns, and in the long term, it could lead to skin cancer [15-20]. On the other hand, it should be noted that UVA radiation is used to treat certain dermatological diseases such as psoriasis, atopic dermatitis and mycosis fungoides, among others [21-25], or for aesthetic purposes, such as in tanning beds [26-28]. In such cases, the radiation is used while taking precautions with regard to the duration of exposure to solar radiation. It is important to be able to analyze changes to the skin, primarily caused by UVB radiation, and there are multiple options to do so. One is the use of non-invasive optical techniques, such as confocal laser microscopy [29, 30], optical coherence tomography [31-36], digital holographic interferometry (DHI) and digital speckle pattern interferometry (DSPI) [37-39]. At present, laser interferometry is a non-destructive and non-invasive optical technique that allows a sample to be analyzed without manipulation. This ensures that the measurements are not altered, thus producing highly accurate results. Laser interferometry uses the phenomenon of interference and monochromatic light sources, such as lasers, to measure displacements, deformations, shapes, vibrations, distances, and refractive indices, among other parameters. It is important to note that laser interferometry is a two-state technique. This means that it is necessary to capture an image without deformation and/or load, which is called a reference, and a second image with a disturbed state (with a modification in the sample). In the present study, we propose using an optical interferometric technique to examine a biological sample before and after exposure to UVB radiation in order to demonstrate its elasticity variations. We will present images of the optical phase, as well as the quantification of the displacements and the change in fringe patterns. Changes in displacement are used to indicate the variation in elasticity that the sample undergoes due to radiation.

2. Optical method and experimental setup

Laser interferometry is a non-destructive optical technique that allows one to analyze a sample without manipulation, yielding highly accurate measurements. To analyze the biological sample, an optical setup based on laser interferometry was required. Figure 1 shows the optical configuration based on the interference phenomenon. The optical configuration includes a Cobolt Samba laser source with a wavelength of 532 nm, and a power output of 1 W. The laser beam is directed towards a beam splitter (BS), which separates it into two beams: the reference beam and the object beam. To avoid illumination loss, both beams are coupled to single-mode optical fibers (FO1 and FO2). The object beam's optical fiber output (FO2) illuminates the sample under study. The backscattered light is collected by an aperture and lens system, and then sent to a combiner cube (CC), where it is merged with the reference beam (FO1). The two beams are then recombined, producing wave superposition and generating an interference pattern [40-43], and the overlap of those two beams is captured by the camera sensor; the camera used was a PCO pixelfly with a resolution of 800 x 600 pixels. To perform the interferometric measurements, an acoustic load (sinusoidal sound waves) was applied to the sample by placing a loudspeaker behind it [44]. This was controlled by a function generator (GF), which allowed controlling the type of signal, as well as the frequency, amplitude and phase, see Fig. 1. In order to discover the characteristic vibration modes in response to the application of sound load, a frequency sweep was performed on the sample, and with the help of a homemade interface, it was possible to visualize its behavior and identify the vibration modes in real time to confirm that the sample was responding effectively. This stage of the experiment was vital in order to obtain the fringe patterns in response to sound and observe the changes due to the UVB radiation.

To record a digital speckle pattern or hologram, the object and reference beams must be recorded simultaneously on the camera sensor using the setup shown in Fig. 1. The intensity of the recorded hologram can be expressed as follows:

$$I(x,y) = a(x,y) + b(x,y)cos[\Delta\phi(x,y)]. \tag{1}$$

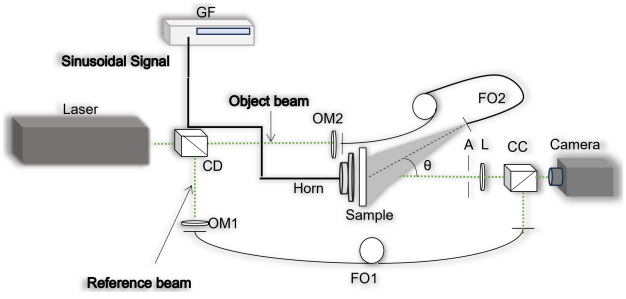


FIGURE 1. Optical setup.

where a, b y $\Delta\phi$ are the background signal, modulation and phase difference, respectively. The latter contains information about the object under study in the form of interference patterns.

In order to find out the fringe vibration pattern of the sample, *i.e.*, to identify its characteristic vibration mode, the sample was subjected to acoustic sound from the rear. To achieve this, it was necessary to record two holograms: one without (I_R) and another with (I_V) the acoustic load. Here, I_R is the so-called reference hologram, which is subtracted from I_V in order to obtain the fringe pattern, showing the intensity modulation by means of:

$$I_F = |I_V - I_R| \tag{2}$$

Subsequently, the optical phase can be recovered from the fringe patterns using the spatial carrier method, which involves the Fourier transform [45-47]. To quantify the displacements $(w(x,y))$ on a micrometric scale the next relationship is used,

$$w(x,y) = \frac{\lambda}{2\pi(1+cos\theta)}\Delta\varphi \tag{3}$$

where $\Delta\varphi$ is the unwrapped optical phase difference, λ is the wavelength of the illumination source used in the optical system, and θ is the illumination angle existing between the observation and illumination directions.

It is important to note that the above process is followed to study samples with and without the exposure to UVB radiation.

3. Results and analysis

Numerous tests were performed to corroborate the repeatability of the process. It is important to note that the biological sample had an uneven thickness and a diameter of 20 mm, which it was placed in an optomechanical circular support. As mentioned before, a frequency sweep was performed to identify the resonant frequencies of the sample, and an interesting finding was that more than two vibration modes were identified, which points to the elasticity of the sample. Before the exposure to UV radiation, the sample was placed in the position displayed in Fig. 1, and two images were captured: one before and another after the application of sound to the sample; it is important to note that the same process is to be followed when UV radiation is applied to the sample.

First, the first vibration mode was obtained using Eq. (2); subsequently, the wrapped phase, unwrapped phase, and displacement maps are obtained [48-53]. Figure 2a) presents the fringe pattern obtained at a frequency of 850 Hz before the application of radiation, while Fig. 2b) shows the fringe pattern when the sample was subjected to a UVB radiation dose of 0.0014 J/cm^2. The vibration frequency of the first mode of the sample remained the same, but it is noticeable that the vibration pattern underwent minor changes, such as a slight rotation of the fringe observed in Fig. 2a), *i.e.*, the

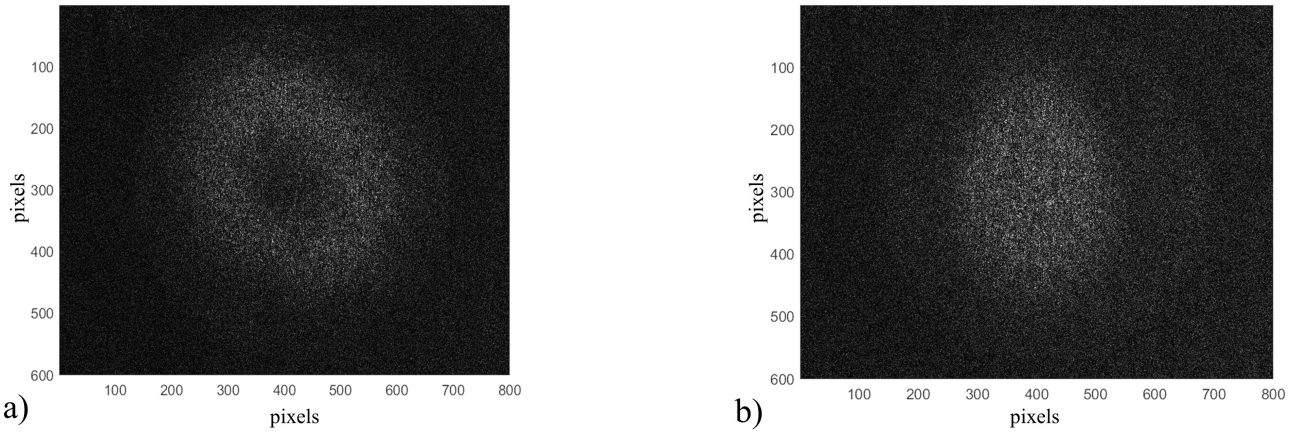


FIGURE 2. Vibration pattern to 850 Hz for the biological sample: a) before and b) after UVB radiation. A slight modification in the fringe pattern is noticeable.

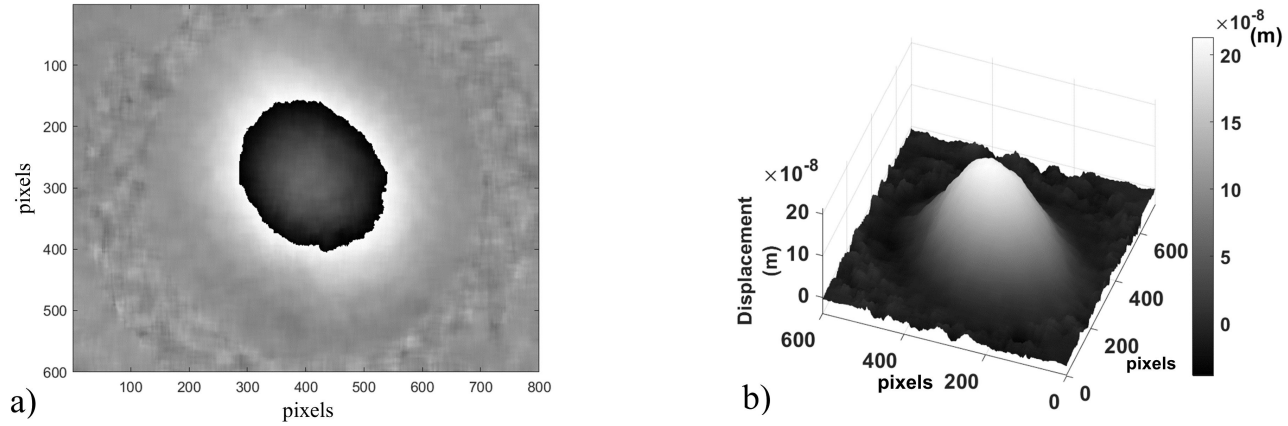


FIGURE 3. Biological sample before UVB radiation, a) wrapped phase and b) displacement map.

fringe appears slightly tilted. In addition, the fringe in Fig. 2a) has dark and bright fringes, while in Fig. 2b) only a bright fringe is visible. This finding suggests that, under the same sound load conditions, the initiation of fringe formation occurs prior to the onset of visible signs of damage, thereby providing an indirect indication of sample elasticity loss after radiation.

A Fourier transform method was applied to the images shown in Fig. 2 to obtain the object's optical phase information; Fig. 3a) presents the wrapped phase, and the displacement map is displayed in Fig. 3b). It is important to mention that the images in Fig. 3 were obtained without using UVB radiation. Meanwhile, Fig. 4 presents the results after the sample had been irradiated; Figs. 4a) and 4b) present the wrapped phase and the displacement map, respectively. To obtain the displacement map shown in Figs. 3b) and 4b), Eq. (3) was used, which depends on the value of λ used, the value of the angle between the observation and illumination directions, θ measured in the optical array, and the unwrapped phase map, $\Delta\varphi$; from these maps, the maximum displacements of the object before and after the application of the radiation dose were obtained and used to construct Table I. The displacement value decreased after UVB irradiation indicating that the sample loses elasticity, *i.e*. the sample is more rigid than at the beginning of the test, when it was in its initial state (without radiation). The displacement value decreased after UVB irradiation, indicating that the sample lost elasticity, *i.e.*, the rigidity increased in the sample compared to the data obtained in its initial state (without radiation).

Analyzing Figs. 3a) and 4b), slight changes in the wrapped phase map are observed. For example, in Fig. 3a), the black fringe is oval and tilted shape, while in Fig. 4a) the dark fringe is smaller than the fringe in Figs. 3a) and it is not tilted. Furthermore, the scale bar in Fig. 3b) is a bit larger compared to Fig. 4b), indicating that the displacement value decreased when the biological sample was subjected to UV radiation, and this is confirmed with the data of Table I, where the maximum displacement of the sample irradiated with UV

TABLE I. Maximum displacement for the first vibration mode found at 850 Hz.

Without UVB radiation	With UVB radiation
0.210 ± 0.015 μm	0.160 ± 0.010 μm

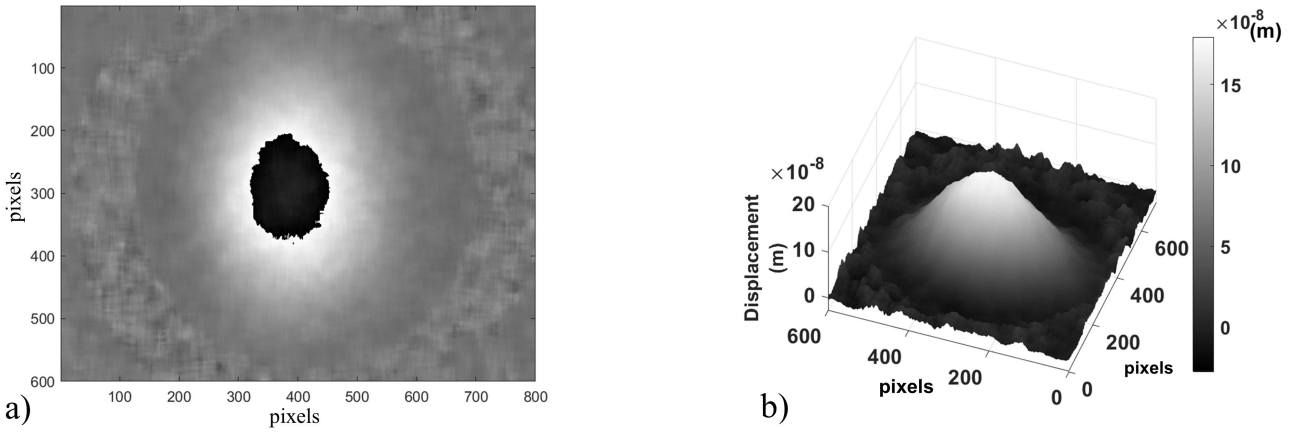


FIGURE 4. Biological sample after application of a UVB radiation dose of 0.0014 J/cm^2, a) wrapped phase and b) displacement map.

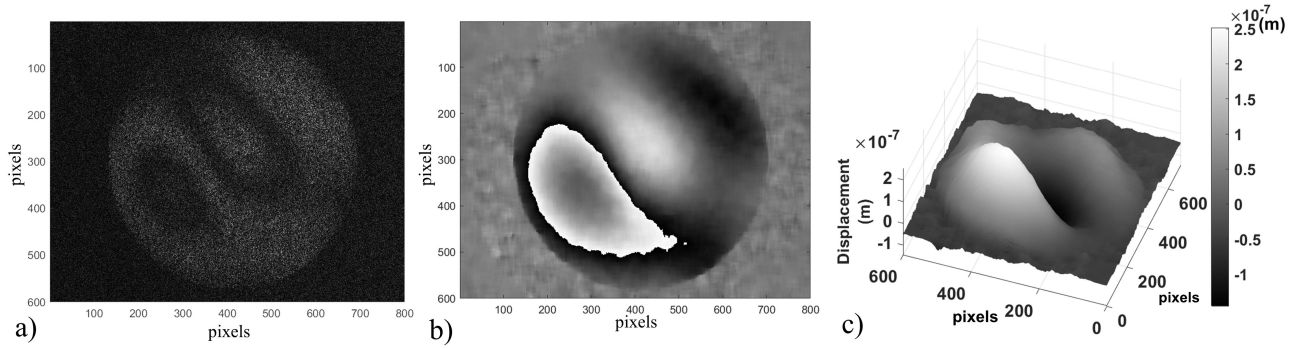


FIGURE 5. Biological sample at a frequency of 1 kHz and without UVB radiation, a) vibration pattern, b) wrapped phase, and c) displacement map.

rays is lower than that of the sample without UV radiation. This assertion is substantiated by the data presented in Table I, which reveals that the maximum displacement of the UVB-irradiated sample is less pronounced than that of the sample not exposed to UVB radiation.

On the other hand, it is important to note that the difference of displacement between sample data with and without UVB radiation is small, exactly 0.05 ± 0.018 μm, due to the low dose of UVB radiation applied to the tissue. If the UVB radiation had been higher, the difference in displacement would have been greater, which could indicate greater damage caused by radiation.

According to the literature, the increased rigidity in biological tissue is associated with higher frequencies and, consequently, lower displacements. Conversely, softer or elastic skin results in lower frequencies, and therefore, greater deformations. Viscoelasticity also plays a role in the tests, as it dampens the sinusoidal signal, leading to modifications in the vibration modes. Another important factor is tissue hydration; as the sample dehydrates, it loses elasticity, which increases its stiffness [54-58]. Thus, after irradiation of the sample with UVB rays, a change occurred in the biological tissue that caused dehydration and/or aging, which caused the displacement values to change for the same frequency.

Another vibration pattern was found at a frequency of 1 kHz. The results obtained when sound was applied to the sample are presented in Fig. 5, without UVB radiation, and 6 with radiation. It is noticeable that the patterns and the displacements are altered upon exposure to the UVB dose. The maximum displacements are shown in Table II.

Examining the vibration pattern images in Figs. 5a) and 6a), the vibration mode appears to be a (1,1) mode, and it is notorious that there are changes in their shapes. For example, in Fig. 5a), bright and dark fringes are presented in a particular position; apparently, the fringes are rotated. However, when the sample is irradiated, the pattern is modified, displaying a pair of dark and bright fringes that are separated and not rotated compared with the pattern without UVB radiation. On the other hand, the displacement maps and the scale bar showed that the displacement value is slightly higher in the sample without radiation, which agrees with the maximum displacement values shown in Table II.

A further result of the experiment was the discovery of a complex vibration pattern found at 1.62 kHz for the sample

TABLE II. Maximum displacements at a frequency of 1 kHz.

Without UVB radiation	With UVB radiation
0.252 ± 0.0014 μm	0.248 ± 0.0011 μm

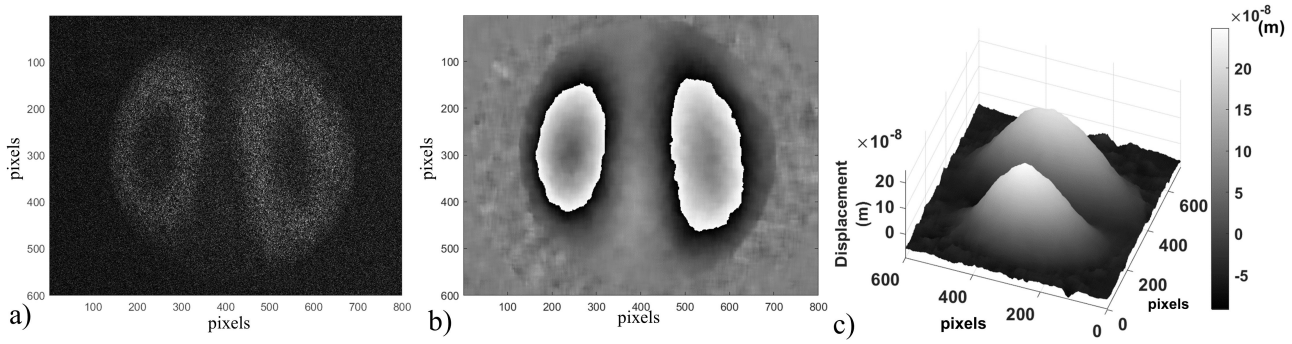


FIGURE 6. Biological sample at a frequency of 1 kHz and with a dose of 0.0014 J/cm^2 of UVB radiation, a) fringe pattern, b) wrapped phase, and c) displacement map.

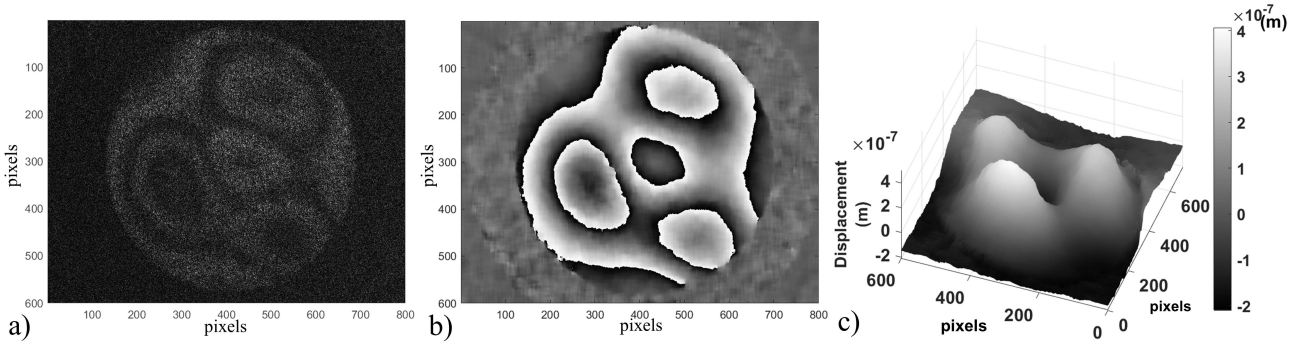


FIGURE 7. Biological sample at a frequency of 1.62 KHz and without UV radiation, a) fringe pattern, b) wrapped phase, and c) displacement map.

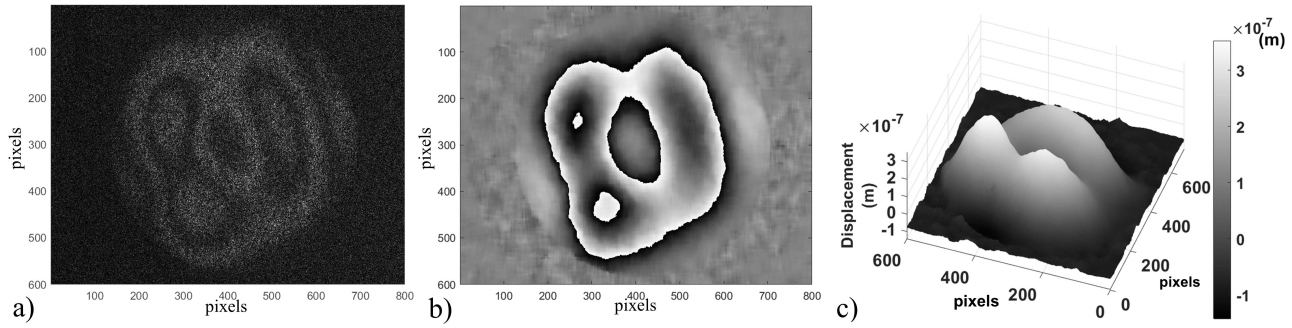


FIGURE 8. Biological sample with a UVB radiation at a frequency of 1.75 KHz, a) fringe pattern, b) wrapped phase, and c) displacement map.

prior to exposure to radiation, as illustrated in Fig. 7. However, following the application of UVB radiation to the sample, it was inspected at 1.62 kHz and did not vibrate at this frequency. Consequently, an exhaustive search for the vibration pattern was carried out, which was found at 1.75 kHz. This indicates that there was a change in frequency, as well as a decrease in the magnitude of the displacement, which is an indicator that the sample is affected after being irradiated, as illustrated in Fig. 8.

A maximum displacement of 0.407 ± 0.0013 μm was quantified for the biological sample without UVB radiation at 1.62 kHz, and a maximum displacement of 0.350 ± 0.0012 μm was determined for the biological sample with UVB radiation dose at a frequency of 1.75 kHz.

The vibration frequency of biological tissue depends on the mechanical properties inherent to its viscoelastic nature. It is worth noting that the biological sample used in this work exhibited various vibration modes at different frequencies, indicating that it cannot be considered a homogeneous system and that its internal structure is complex.

In addition, the alteration of the sample with UVB radiation caused slight changes in the displacement information and the vibration patterns detected by optical techniques.

4. Conclusions

The research presented allowed us to analyze biological tissue using a non-invasive optical technique, which facilitated

the quantification of micro-displacements and changes in them caused by UVB radiation applied to the sample. The laser interferometry technique permitted the biological sample to be evaluated without manipulation, which helped to avoid external alterations that could influence the measurements. Furthermore, the optical technique used in this work lets us see superficial variations and/or modifications in the biological sample that are not perceptible to the naked eyed. In this regard, changes in the outer layer of the sample due to UVB radiation can be seen in the 3D displacement maps.

It was imperative to discover the vibration modes of the tissue prior to its quantitative analysis, and consequently, tissue information was obtained and analyzed before and after UVB radiation. The displacement in the tissue before UVB radiation was greater in comparison to the displacement values obtained with the irradiated sample; additionally, when the sample was subjected to UVB radiation, the fringe patterns and elasticity were modified, as UVB rays generate an increase in viscoelastic stiffness on the tissue surface, indicating photoaging and dehydration, as well as possible internal alterations in elastin, fragmentation, and collagen reorganization [15]. Thus, in the first and second vibration modes found, the frequency of the sound load at which they were found remained the same for both sample conditions with and without radiation. However, the behavior of the phase and displacement maps changed, and a decrease in the displacement values of the irradiated sample was observed. In a complex vibration pattern, in addition to the change in displacement, the frequency also changed from 1.62 kHz to 1.75 kHz due to the effects of UVB radiation on the tissue.

It should be noted that the difference in maximum displacement between the irradiated and non-irradiated samples was small due to the low dose of radiation that was applied; these small changes of the order of microns can be detected with the technique presented. In future work, focus will be on obtaining mechanical parameters such as stiffness, Young's modulus, and Poisson's ratio, among others, in order to better understand the damage that prolonged exposure to UVB rays can cause to human skin.

Acknowledgments

The authors acknowledge support from their institution.

1. US EPA, O. (2015) Sun safety, US EPA. Available at: https://www.epa.gov/sunsafety, (Consulted: december 12th, 2025).
2. El deterioro de la capa de ozono, problema vigente (2019). Gaceta UNAM.
3. Agotamiento de la capa de ozono (2019) National Geographic. Available at: https://www.nationalgeographicla.com/espacio/2019/01/agotamiento-de-la-capa-de-ozono, (Consulted: december 12th, 2025).
4. F. López Figueroa, Implicaciones dermatológicas del cambio climático y de la disminución de la capa de ozono, *Actas Dermo-Sifiliográficas*, **102** (2011), 311-315, https://doi.org/10.1016/j.ad.2010.12.006.
5. S. A. Umar and S. A. Tasduq, Ozone Layer Depletion and Emerging Public Health Concerns - An Update on Epidemiological Perspective of the Ambivalent Effects of Ultraviolet Radiation Exposure, *Front. Oncol.*, **12**, (2022), 1-11, https://doi.org/10.3389/fonc.2022.866733.
6. K. R. Solomon, Effects of ozone depletion and UV-B radiation on humans and the environment, Atmosphere-Ocean, **46** (2008) 185-202, https://doi.org/10.3137/ao.460109.
7. E Kovács, and Á Keresztes, Effect of gamma and UV-B/C radiation on plant cells, Micron, **33** (2002) 199-210, https://doi.org/10.1016/S0968-4328(01)00012-9.
8. A. L. Andrady, A. M. Heikkilä, K. K. Pandey, L. S. Bruckman, C. C. White, M. Zhu, and L. Zhu, Effects of UV radiation on natural and synthetic materials. *Photochem Photobiol Sci*, **22** (2023) 1177-1202, https://doi.org/10.1007/s43630-023-00377-6.
9. M. M. Shokrieh, and A. Bayat, Effects of Ultraviolet Radiation on Mechanical Properties of Glass/Polyester Composites. Journal of Composite Materials, **41** (2007) 2443-2455, https://doi.org/10.1177/0021998307075441.
10. A. Leal-Junior, R. Pires-Junior, A. Frizera, and C. A. F. Marques, (2022). Influence of UV radiation on mechanical properties of polymer optical fibers, *Polymers*, **14** (2022), 4496, https://doi.org/10.3390/polym14214496.
11. R. Naveen, M. Kumar, M. Ramesh, R. Abinaya, and M. S. Prasath, An investigation on effect of ultraviolet (UV) rays on mechanical properties of epoxy laminates, Materials Today: Proceedings, (2023), https://doi.org/10.1016/j.matpr.2023.06.257.
12. S. Muñoz Solís, M. S. Hernández-Montes, and F. Mendoza Santoyo, Measurement of Young's modulus in an elastic material using 3D digital holographic interferometry, *Appl. Opt.*, **50**, (2011), 3383-3388.
13. S. Eve, and J. Mohr, Effects of UV-irradiation on the thermo-mechanical properties of optical grade poly(methyl methacrylate), *Applied Surface Science*, **256** (2010), 2927-2933, https://doi.org/10.1016/j.apsusc.2009.11.052.
14. L. Silva Acosta, M. S. Hernández-Montes, F. Mendoza Santoyo, M. H. De la Torre, J. M. Flores, G. Frausto, and S. Muñoz, Study of skin rigidity variations due to UV radiation using digital holographic interferometry, *Opt. Lasers Eng.*, **126** (2020) 105909.
15. R. P. Gallagher and T. K. Lee, Adverse effects of ultraviolet radiation: A brief review, *Progress in Biophysics and Molecular Biology*, **92**, (2006), 119-131, https://doi.org/10.1016/j.pbiomolbio.2006.02.011.

16. D'Orazio, S. Jarrett, A. Amaro-Ortiz and T. Scott, UV radiation and the skin. *Int. J. Mol. Sci.*, **14** (2013), 12222-12248, https://doi.org/10.3390/ijms140612222.

17. R.P. Gallagher, T. K. Lee, C. D. Bajdik and M. Borugian, Ultraviolet radiation. *Chronic Dis Can.*, **29** (2010), 51-68, https://doi.org/10.24095/hpcdp.29.S1.04.

18. C. Nishigori, N. Yamano, M. Kunisada, A. Nishiaki-Sawada, H. Ohashi and T. Igarashi, Biological Impact of Shorter Wavelength Ultraviolet Radiation-, *Photochemistry y Photobiology*, **99** (2023), 335-343, https://doi.org/10.1111/php.13742.

19. K. A. Merin, M. Shaji, and R. Kameswaran, A review on sun exposure and skin diseases, *Indian Journal of Dermatology*, **67** (2022), 625, https://doi.org/10.4103/ijd.ijd_1092_20.

20. F. Papaccio, S. Caputo and B. Bellei, Focus on the contribution of oxidative stress in skin aging. *Antioxidants*, **11** (2022) 1121, https://doi.org/10.3390/antiox11061121.

21. S. L. Yu, and S. K. Lee, Ultraviolet radiation: DNA damage, repair, and human disorders, *Mol. Cell. Toxicol.*, **13**, (2017), 21-28, https://doi.org/10.1007/s13273-017-0002-0.

22. C. Green, B. L. Diffey and J. L. M. Hawk, Ultraviolet radiation in the treatment of skin disease, *Physics in Medicine and Biology*, **37** (1992), 1-20, https://doi.org/10.1088/0031-9155/37/1/001.

23. E. B. M. Kroft, N. J. G. Berkhof, P. C. M. van de Kerkhof, R. M. J. P. Gerritsen and E. M. G. J. de Jong, Ultraviolet A phototherapy for sclerotic skin diseases: A systematic review, *Journal of the American Academy of Dermatology*, **59** (2008), 1017-1030, https://doi.org/10.1016/j.jaad.2008.07.042.

24. F. Breuckmann, T. Gambichler, P. Altmeyer and A. Kreuter, UVA/UVA1 phototherapy and PUVA photochemotherapy in connective tissue diseases and related disorders: a research based review, BMC Dermatol, **4** (2004), 1-14, https://doi.org/10.1186/1471-5945-4-11.

25. M. Šitum, V. Bulat, K. Majcen, A. Džapo and J. Ježovita, Benefits of Controlled Ultraviolet Radiation in the Treatment of Dermatological Diseases, *Coll. Antropol*, **38** (2014) 1249-1253.

26. W. L. Scarlett, Ultraviolet radiation: sun exposure, tanning beds, and vitamin D levels. What you need to know and how to decrease the risk of skin cancer, *JAOA.*, **103** (2003), 371-375, https://doi.org/10.7556/jaoa.2003.103.8.371.

27. R. P. Gallagher, J. J. Spinelli and T. K. Lee, Tanning Beds, Sunlamps, and Risk of Cutaneous Malignant Melanoma, *Cancer Epidemiol Biomarkers Prev.*, **14**((2004), 562-566, https://doi.org/10.1158/1055-9965.EPI-04-0564.

28. K. P. Radack, M. E. Farhangian, K. L. Anderson and S. E. Feldman, A Review of the Use of Tanning Beds as a Dermatological Treatment, *Dermatol Ther (Heidelb)*, **5** (2015) 37-51, https://doi.org/10.1007/s13555-015-0071-8.

29. A. Gerger, S. Koller, T. Kern, C. Massone, K. Steiger, E. Richtig, H. Kerl, and J. Smolle, Diagnostic Applicability of In Vivo Confocal Laser Scanning Microscopy in Melanocytic Skin Tumors, *Journal of Investigative Dermatology*, **124** (2005) 493-498, https://doi.org/10.1111/j.0022-202X.2004.23569.x.

30. M. A. Ilie, C. Caruntu, M. Lupu, D. Lixandru, M. Tampa, S-R. Georgescu, A. Bastian, C. Constantin, M. Neagu, S. Andrada Zurac, and D. Boda, Current and future applications of confocal laser scanning microscopy imaging in skin oncology (Review), *Oncology Letters*, **17** (2019), 4102-4111, https://doi.org/10.3892/ol.2019.10066.

31. O. Babalola, A. Mamalis, H. Lev-Tov, and J. Jagdeo, Optical coherence tomography (OCT) of collagen in normal skin and skin fibrosis. *Arch Dermatol Res*, **306**, (2014), 1-9, https://doi.org/10.1007/s00403-013-1417-7.

32. M. Mogensen, L. Thrane, T.M. Joergensen, P.E. Andersen, and G.B.E. Jemec, Optical Coherence Tomography for Imaging of Skin and Skin Diseases, *Annals of Clinical Psychiatry*, **28** (2016), 196-202, https://doi.org/10.1177/104012371602800309.

33. J. Welzel, Optical coherence tomography in dermatology: a review, *Skin Research and Technology*, **7** (2001) 1-9, https://doi.org/10.1034/j.1600-0846.2001.007001001.x.

34. K. V. Larin and D. D. Sampson, Optical coherence elastography - OCT at work in tissue biomechanics [Invited], *Biomedical Optics Express*, **8** (2017) 1172-1202, https://doi.org/10.1364/BOE.8.001172.

35. J. Rogowska, N. Patel, S. Plummer, and M. E. Brezinski, Quantitative optical coherence tomographic elastography: method for assessing arterial mechanical properties, *British Journal of Radiology*, **79** (2006) 707-711, https://doi.org/10.1259/bjr/22522280.

36. I. A. Sigal, J. L. Grimm, J. S. Schuman, L. Kagemann, H. Ishikawa, and G. Wollstein, A Method to Estimate Biomechanics and Mechanical Properties of Optic Nerve Head Tissues From Parameters Measurable Using Optical Coherence Tomography. *IEEE Transactions on Medical Imaging*, **33** (2014) 1381-1389, https://doi.org/10.1109/TMI.2014.2312133.

37. D. S. Zhang, and D. D. Arola, Applications of digital image correlation to biological tissues, *Journal of Biomedical Optics*, **9** (2004), 691-699, https://doi.org/10.1117/1.1753270.

38. G. Pedrini, I. Alexeenko, P. Zaslansky, H. J. Tiziani, and Wolfgang Osten, Digital holographic interferometry for investigations in biomechanics, Proc. SPIE 5776, *Eighth International Symposium on Laser Metrology*, (2005) 325-332, https://doi.org/10.1117/12.611633.

39. L. Silva Acosta, F. Mendoza Santoyo, J. M. Flores, M. S. Hernández-Montes, M. H. De la Torre, G. Frausto, S. Muñoz, and E. E. Lozada, Study of skin aging effects induced by near UV radiation using time average digital holographic interferometry, *Opt. Lasers Eng.*, **137**, (2020), 106345.

40. P. K. Rastogi, Holographic Interferometry Principles and Methods. Springer Series in Optical Sciences, 1st edition, (1994) 7-32, https://doi.org/10.1007/978-3-540-48078-5.

41. G. H. Kauffmann, Advances in Speckle Metrology and Related Techniques, Wiley-VCH, (2011).

42. S. S. Andrews, Light and Waves: A Conceptual Exploration of Physics, Springer Nature Switzerland, (2023) 43-70.
43. K. J. Gasvik, Optical metrology. John Wiley & Sons, Ltd, (2002), 37-65.
44. J. Clinton, and K. P. Wani, Extracting Vibration Characteristics and Performing Sound Synthesis of Acoustic Guitar to Analyze Inharmonicity, *Open Journal of Acoustics*, **10** (2020), 41-50, https://doi.org/10.4236/oja.2020.103003.
45. M. Takeda, H. Ina, y S. Kobayashi, Fourier-transform method of fringe-pattern analysis for computer-based topography and interferometry, *J. Opt. Soc. Am*, **72**(1), (1982), 156-160, https://doi.org/10.1364/JOSA.72.000156
46. Y. I. Ostrovsky, V. P. Shchepinov, and V. V. Yakovlev, Holographic interferometry, in Holographic Interferometry in Experimental Mechanics, Springer Series in Optical Sciences, 1st edition, **Vol. 60**, Springer, Berlin, Heidelberg, (1991), 24-87.
47. T. Kreis, Handbook of Holographic Interferometry: Optical and Digital Methods, Wiley, (2004), 185-218.
48. M. Servin, J. A. Quiroga and M. Padilla, Fringe Pattern Analysis for Optical Metrology: Theory, algorithms and applications, Wiley, (2014).
49. S. Zhang, Composite phase-shifting algorithm for absolute phase measurement. *Opt. Laser Eng.*, **50** (2012), 1538-1541, https://doi.org/10.1016/j.optlaseng.2012.06.005.
50. K. Itoh, Analysis of the Phase Unwrapping algorithm, *Appl. Opt.*, **21** (1982), 2470, https://doi.org/10.1364/AO.21.002470.
51. J. M. Huntley, Noise Immune Phase Unwrapping Algorithms, *Appl. Opt.*, **28** (1989), 3268-3270, https://doi.org/10.1364/AO.28.003268.
52. J. M. Huntley, and J. R. Buckland, Characterization of sources of 2π discontinuities in speckle interferograms, *J. Opt. Soc. Am. A*, **12** (1995), 1990-1996, https://doi.org/10.1364/JOSAA.12.001990.
53. D. C. Ghiglia, and L. A. Romero, Minimum Lp-Norm Two-Dimensional Phase Unwrapping, *J. Opt. Soc. Am. A*, **13** (1996), 1999-2013, https://doi.org/10.1364/JOSAA.13.001999.
54. K. Moon Jeong, K. Bo-seung, H. Sejin, and Y. Hong Hee, Experimentally derived viscoelastic properties of human skin and muscle in vitro, *Medical Engineering & Physics*, **61** (2018) 25-31, https://doi.org/10.1016/j.medengphy.2018.08.001.
55. S. Sakaguchi, and M. Konyo, Skin viscoelasticity effects on the periodic mechanical stimuli propagation between skin layers. *Journal of the Mechanical Behavior of Biomedical Materials.* **152**, (2024), 106416, https://doi.org/10.1016/j.jmbbm.2024.106416.
56. M. L. Crichton, X. Chen, H. Huang, M. A.F. Kendall, Elastic modulus and viscoelastic properties of full thickness skin characterised at micro scales, *Biomaterials*, **34** (2013), 2087-2097, https://doi.org/10.1016/j.biomaterials.2012.11.035.
57. H. Koruk, and S. Rajagopal, A Comprehensive Review on the Viscoelastic Parameters Used for Engineering Materials, Including Soft Materials, and the Relationships between Different Damping Parameters, *Sensors (Basel)*, **24** (2024) 6137, https://doi.org/10.3390/s24186137.
58. R. Lakes, Viscoelastic Materials, Cambridge University Press, (2009), 236-237, 341-376.